Law of the wall for small-scale streamwise turbulence intensity in high-Reynolds-number turbulent boundary layers

B. Ganapathisubramani*
University of Southampton, Southampton SO17 1BJ, United Kingdom

(Received 22 May 2018; published 31 October 2018)

Following the dimensional analysis approach carried out in previous studies, it is hypothesized that the small-scale fluctuations should only depend on the inner scales, analogous to the Prandtl's law of the wall for the mean flow. This allows us to examine the high-frequency regime of the streamwise energy spectra where a "law of the wall" in spectra would hold. Observations in high-Reynolds-number turbulent boundary layer data indicate that a conservative estimate for the start of this law of the wall is $f^+ = 0.005$ (which corresponds to 200 viscous time units) across a range of wall-normal positions and Reynolds numbers. This is sufficient to capture the energetic viscous-scaled motions such as the near-wall streaks, which have a timescale of approximately 100 viscous units. This spectral collapse is consistent with the observations in internal flows and external flows in other studies. Furthermore, the spectral collapse leads to a universal scaling (based on skin-friction velocity and kinematic viscosity) for the small-scale streamwise turbulence variance (consistent with the hypothesis) across the entire boundary layer. A logarithmic variation of this small-scale variance is observed farther away from the wall.

DOI: 10.1103/PhysRevFluids.3.104607

I. BACKGROUND

A number of previous efforts have focussed on proposing scaling laws for turbulent energy spectra of turbulent wall flows. Perry and Abell [1] was perhaps the first to develop scaling laws for streamwise energy spectra using dimensional analysis approach. This work has been extensively extended in various subsequent studies [2–4]. The primary focus of these efforts were on the overlap scaling of streamwise energy spectra where the energy content is inversely proportional to the wall-normal position. The choice of different velocity and length scales for the dimensional analysis in these previous studies were underpinned by the attached-eddy hypothesis, a model of wall turbulence that provides critical insights. Very recently, Zamalloa *et al.* [5] used dimensional analysis and proposed "model-free" scaling relations for the turbulent-energy spectra in different regions (near-wall, log, and outer wake regions) of turbulent wall flows. Specifically, they demonstrated the presence of law of the wall in the high-wave-number regime of energy spectra in pipe and channel flows using experimental and DNS data over a limited range of Reynolds numbers.

In this paper, we present a reinterpretation of the dimensional analysis work carried out by Perry and Abell [1] and Zamalloa *et al.* [5] as well as observations of law of the wall in small-scale turbulence intensity and in the high-frequency regime of streamwise energy spectra in high-Reynolds-number turbulent boundary layers. We highlight some subtle differences (compared to those previous studies) in the choice of velocity and length scales (used in dimensional analysis) and justify these choices based on physical reasoning and experimental observations.

*g.bharath@soton.ac.uk

II. LAW OF THE WALL FOR STREAMWISE ENERGY SPECTRA

This section is a recap of the dimensional analysis performed in Refs. [1,5]. However, we highlight the choice of different scaling variables and the reasoning required for it. Let $\phi_{11}(k_1, y)$ be the power spectral density of the streamwise velocity fluctuation for a longitudinal wave number k_1 at location y away from the wall. Then, the integral over all k_1 of this power spectral density is equal to the turbulent energy of the streamwise velocity component at that wall-normal location:

$$\int_0^\infty \phi_{11}(k_1, y)dk_1 = u^2(y). \tag{1}$$

Now, $k_1\phi_{11}(k_1, y)$ is the turbulent energy contained at a given wave number k_1 at a certain wall-normal location. Following Refs. [1,5] and their dimensional analysis approach, it is clear that we need a velocity scale to nondimensionalize $k_1\phi_{11}$ and potentially two different length scales for the wave number and wall-normal position:

$$\frac{k_1\phi_{11}(k_1, y)}{\tilde{U}^2} = F(kL_1, y/L_2), \tag{2}$$

where L_1 is the relevant length scale for the wave number and L_2 is the relevant length scale for the wall-normal position. $\tilde{U}$ is the relevant velocity scale for the energy. We have to use physical arguments to arrive at appropriate choices for these scales.

Recall that Prandtl's law of the wall for mean flow postulates that at high Reynolds numbers, close to the wall ($y \ll \delta$, where δ is the outer length scale), there is an inner layer in which the mean velocity is determined by the viscous scales, independent of outer length and velocity scales. Based on this, we arrive at an equation for the mean flow, which is the law of the wall:

$$\frac{U}{U_\tau} = f_w\left(\frac{yU_\tau}{\nu}\right) \tag{3}$$

U_τ is the skin-friction velocity ($U_\tau = \sqrt{\tau_w/\rho}$, where τ_w is the wall-shear stress and ρ is the density of the fluid) and ν is the kinematic viscosity of the fluid.

We can follow the same reasoning as for the mean profile to determine the appropriate values for $\tilde{U}$, L_1, and L_2. As an observer at the wall with "no knowledge" of the outer flow, there is only one choice for $\tilde{U}$, which is the viscous velocity scale (U_τ). There may be two possible candidates for L_1: viscous length scale (ν/U_τ) and wall-normal position (y). For L_2, there is only one possible candidate, which is the viscous length scale ν/U_τ (note that we will represent scales nondimensionalized with the viscous scales with a superscript "+"). Then, the spectral scaling becomes

$$\frac{k_1\phi_{11}(k_1, y)}{U_\tau^2} = F(k_1L_1, y^+). \tag{4}$$

The authors of Ref. [1] used their insights from attached-eddy hypothesis and chose $L_1 = y$ that highlights distance from the wall scaling. They used U_τ to be the velocity scale. Here, we take a different approach to determine L_1. We postulate that there exists a law of the wall for the small-scale velocity fluctuations, i.e., the integral of the spectrum over a certain high-wave-number range. In the near-wall region, the variance of the small scales over a range of high wave numbers is only influenced by inner velocity scale such that

$$\frac{\overline{u_S^2}}{U_\tau^2} = g_w(y^+), \tag{5}$$

where u_S^2 is the variance of the streamwise velocity fluctuations in the high-wave-number regime that should conform to law of the wall and g_w is the function that represents law of the wall for these small-scale motions. This will result in a universal form that is only dependent on viscous scales and is independent of outer influence. Therefore, we can choose L_1 as ν/U_τ. For these high

wave numbers, Ref. [1] used the classical Kolmogorov scaling of η (length scale) and v_η (velocity scale) that depends on the dissipation of turbulent kinetic energy ($\langle\epsilon\rangle$). However, given that the Kolmogorov scales changes with wall-normal direction, especially in the near-wall region, the inner scales are a much more stringent requirement compared to Kolmogorov scales. Additionally, it ensures that the small-scale turbulence intensity has the same scaling parameters as the mean flow.

This assumption is consistent recent observations of the small-scale behavior in wall-bounded flows. Recently, Ref. [6] showed the universality in the small scales across different flows even in low Reynolds numbers. This was especially true farther away from the wall. Reference [7] showed that the kinetic energy dissipation (and the Kolmogrov scale) in the near-wall region of a turbulent channel flow scales with the inner scales. They show excellent collapse of η^+ versus y^+ with increasing Reynolds numbers. Dissipation is a weighted integral of the energy spectrum, where the weighting is toward the higher wave numbers. Therefore, the collapse in small-scale turbulence intensity is similar to the collapse of integrated dissipation spectra. The dissipation-based length scale (i.e., the Kolmgorov scale) provide a good scaling parameter for boundary-free flows; however, in the presence of the wall, skin-friction velocity (U_τ) captures the integrated effects of the large scales and small scales and therefore represents a better scaling parameter. In fact, Ref. [7] built on previous efforts [8,9] and showed that the probability density functions of instantaneous Kolmogorov scale can be collapse with an outer length scale that is derived based on Townsend's attached eddy model. This was necessary to capture the effect of the large scale on the small scales. Based on these arguments, we set L_1 to be ν/U_τ. Therefore,

$$g_w(y^+) = \int_{M^+}^{\infty} F(k_1^+, y^+) d[ln(k_1^+)] \tag{6}$$

is a universal function in the inner region across Reynolds numbers. At fixed values of y^+ close enough to the wall (i.e., $y \ll \delta$), the above equation indicates that there should be a universal value of M^+ that is independent of y^+.

Zamalloa *et al.* [5] use y as their length scale L_1; however, they recognized that this scaling can be replaced with a scaling similar to the one mentioned above. They did not examine this in any detail. They used data and observed that the spectra collapses for high wave numbers, if $k_1 y \geqslant 10(y^+/\mathrm{Re}_\tau)$. This translates to $k_1^+ \geqslant 10/\mathrm{Re}_\tau$ or $k_1\delta \geqslant 10$, which essentially means that there should be one order of magnitude difference in the wave-number range compared to the large scales of the flow. These observations were limited in Reynolds number range (only up to $\mathrm{Re}_\tau \approx 3000$) and were confined to internal flows. This limit of collapse might have an outer influence since the scale separation is not sufficiently large. However, the choice of U_τ as the velocity scale should ensure that there is collapse in the high-wave-number regime. Therefore, it is important to examine this collapse at higher Reynolds numbers to determine if there exists an appropriate wave-number cutoff that eliminates the dependence of distance from the wall (or Reynolds number). This is examined in the next section.

III. OBSERVATIONS IN TURBULENT BOUNDARY LAYERS

It is very difficult to obtain wave-number spectra at high Reynolds numbers without invoking Taylor's hypothesis where we have to assume or model a frequency–wave-number mapping function. Typically, this mapping function is assumed to just depend on the local mean velocity. This could lead to incorrect observations on the nature of collapse of spectra. Therefore, here we resort to using frequency spectra from hot-wire data without invoking Taylor's hypothesis (or other equivalent mapping). In this case, the law of the wall for spectra becomes

$$\frac{f\phi_{11}(f, y)}{U_\tau^2} = F(fT_1, y^+), \tag{7}$$

where f is the frequency and T_1 is a suitable timescale. Following the same arguments as in the previous section, the appropriate timescale should be the inner timescale based on wall-shear

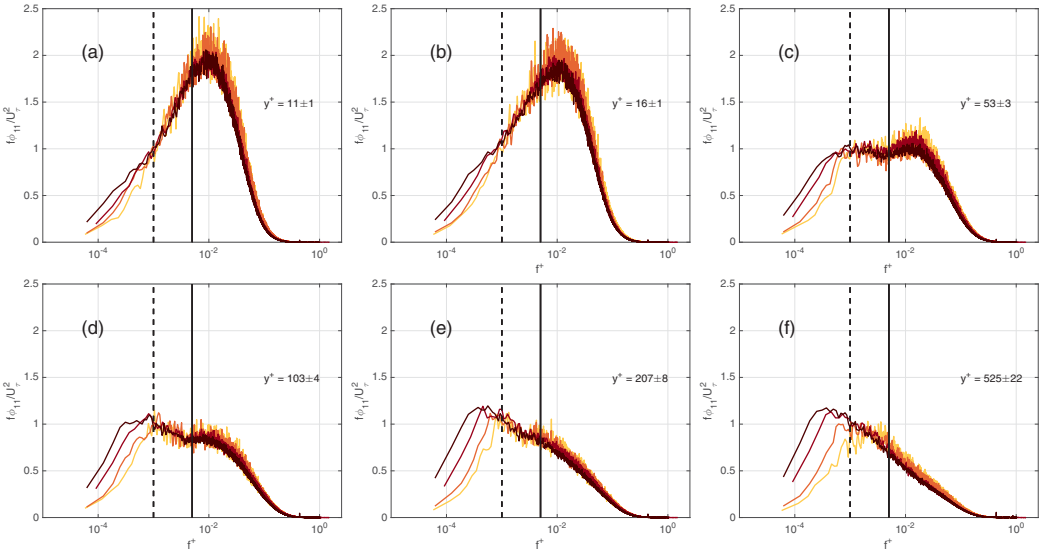

FIG. 1. [(a)–(f)] Inner-normalized energy spectra for four different Reynolds numbers at six different values of y^+. The figures show the value of y^+ and the variance in that selected wall-normal location across the Reynolds numbers. Lines are colored from lightest to darkest in order of increasing Re_τ (= 2800, 3900, 7300, and 14150). The solid black line shows the $f^+ = 0.005$, which is 200 inner time units, while the dashed black line shows $f^+ = 0.001$, which is 1000 inner time units.

stress and viscosity, $T_1 = \nu/U_\tau^2$. This makes the law of the wall for streamwise energy spectrum in frequency domain

$$\frac{f\phi_{11}(f,y)}{U_\tau^2} = F(f^+, y^+). \tag{8}$$

We now seek collapse in spectra across Reynolds numbers such that

$$g_w(y^+) = \frac{u_S^2(y^+)}{U_\tau^2} = \int_{A^+}^{\infty} F(f^+, y^+) d[ln(f^+)] \tag{9}$$

is a universal function in the inner region. Here, A^+ is equivalent to M^+ where at fixed values of y^+ close enough to the wall (i.e., $y \ll \delta$), there is a universal value of A^+.

Hot-wire measurements obtained in Melbourne's high-Reynolds-number boundary-layer wind tunnel (HRNBLWT) is used to compare spectra at similar wall-normal locations over a range of Reynolds numbers (Re_τ = 2800, 3900, 7300, 14150). The datasets for Re_τ = 2800, 3900, and 7300 are obtained from Refs. [10,11]. The dataset for Re_τ = 14150 is from Ref. [12]. Figure 1 shows the energy spectra against inner-normalized frequency over a range of wall-normal locations including $y^+ = 11 \pm 1$, 16 ± 1, 53 ± 3, 103 ± 4, 207 ± 8, and 525 ± 22. The largest y^+ value is chosen to be in outer edge of the log region at the lowest Reynolds number. It is difficult to obtain data at exactly the same y^+ values across different Reynolds numbers. Therefore, the locations mentioned are average of the nearest wall-normal location over the range of Reynolds numbers and the error is based on twice the standard deviation of the wall-normal positions that are chosen across Reynolds numbers.

Spectra in Fig. 1 shows excellent collapse in the spectra at high frequencies where we expect the law of the wall to hold. It should be noted the data at the highest Reynolds number might suffer from mild attenuation of energy due to spatial resolution of the hot-wire probe, especially at these high frequencies [10]. Despite this, the collapse

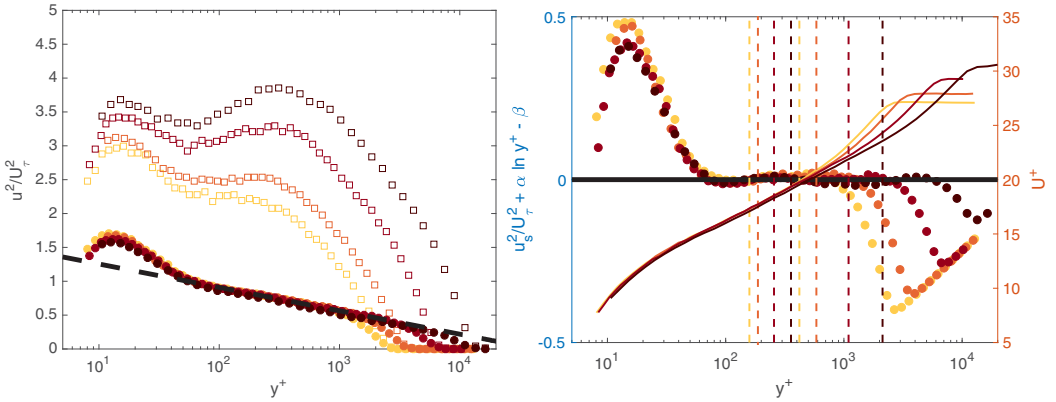

FIG. 2. (Left) Inner normalized large-scale (open squares) and small-scale (filled circles) variance of streamwise velocity for four different Reynolds numbers. The separation between large and small scale is based on a Fourier filter at $f^+ = 0.005$. The dashed black line shows the log decay of the small-scale variance beyond $y^+ > 100$. (Right) Compensated form of small-scale variance where the fitted log trend is subtracted from the data (symbols) and the log region in the mean flow (solid lines). The dashed lines show the extent of log region ($3\sqrt{\mathrm{Re}_\tau} \leqslant y^+ \leqslant 0.15\mathrm{Re}_\tau$). Increasing darkness in all symbols and lines represents increasing Reynolds number.

is obvious even at $y^+ \approx 103$ down to a frequency of $f^+ = 0.001$ (which is shown in dashed line in the figure). Below this frequency, the outer influence becomes obvious and the spectra for each Reynolds number peel off at different frequencies. The quality of the collapse is worse at $y^+ = 525$. At that location, wall-normal location is at the outer edge of the log region at $\mathrm{Re}_\tau = 2800$, while it is still in the log region for the other Reynolds numbers. We expect the law of the wall for the small scales of the spectrum to diminish at these locations where the shear is minimal and therefore the spectra at the small scales would collapse with Kolmogorov scales. Regardless, in the near-wall region (where y^+ is small and $y \ll \delta$), there is excellent collapse in the spectra at least up to $f^+ = 0.005$ (shown as solid black line) and perhaps up to $f^+ = 0.001$ (dashed line).

Based on the above observations, a conservative estimate for A^+ in Eq. (9) can be 0.005. We can now integrate the power spectral density from this value of A^+ up to infinity. This should give the near-wall small-scale turbulent energy, which obeys law of the wall. The amount of energy contained in these scales will diminish farther away from the wall. In fact, farther away from the wall, the viscous scale may no longer be equal to inner scales but could be replaced with Kolmogorov scales, as in Ref. [1]. However, farther away from the wall, it is difficult with current experimental data to delineate if this frequency should scale with viscous wall units or Kolmogorov scales. From balancing production and dissipation in the logarithmic region, authors of Ref. [4] found that the inner-normalized Kolmogorov timescale, t_η^+, should vary as $t_\eta^+ \approx \sqrt{(\kappa y^+)}$ (where κ is the Karman constant). Therefore, the value A^+ in terms of Kolmogorov scales will vary with wall-normal location as $A_\eta \approx 0.005\sqrt{\kappa y^+}$. For the higher Reynolds number considered here, this would translate to $A_\eta \approx 0.06$ (at the lower end of the log region) and $A_\eta \approx 0.14$ (at the upper end of the log region). It is difficult to discern collapse (or lack thereof) with the current data and does not preclude the presence of Kolmogorov scaling. However, it does suggest that inner scaling provides a bound for the low-frequency limit where there is indeed collapse of the small scales (that is consistent with the Kolmogorov scaling).

The impact of using $A^+ = 0.005$ as the cutoff frequency is explored by computing the large-scale and small-scale variances of streamwise velocity based on this cutoff value. Figure 2 shows these two quantities in inner scaling. The small-scale fluctuations across Reynolds numbers collapse across the entire range of wall-normal locations (up to $y^+ \approx 1000$, which is well outside the

log region for the lower Reynolds number). In fact, the small-scale variance appears to follow a logarithmic decay with wall-normal position for $y^+ > 3\sqrt{\mathrm{Re}_\tau}$ across all Reynolds numbers. This logarithmic decay extends well into the outer region (beyond the traditional log region for the mean profile). This log decay has the form

$$\frac{u_S^2(y^+)}{U_\tau^2} = -\alpha \ln(y^+) + \beta \text{ for } y^+ > 3\sqrt{\mathrm{Re}_\tau}, \tag{10}$$

where $\alpha = -0.15 \pm 0.002$ and $\beta = 1.59 \pm 0.01$ [the uncertainty estimates are based on the rms of the difference between the experimental data and Eq. (10) across all Reynolds numbers within the log region as identified in the mean flow].

This log trend is further clarified in Fig. 2 (right) where the small-scale turbulence is plotted in compensated form (i.e., the log trend determined above was subtracted from the data with the given constants). This compensated form is similar to the indicator function (where the gradients are plotted); however, this compensated form is preferred here to avoid numerical differentiation of coarsely sampled (in y direction) experimental data. The figure clearly exhibits a residue of nearly zero over a wide range of wall-normal locations, which is a reflection of the presence of the log region of the above form. The figure also shows the logarithmic region exhibited by the mean flow and dashed lines show a conservative estimate of the log region (at each Reynolds number) in the mean flow following [13], $3\sqrt{\mathrm{Re}_\tau} \leqslant y^+ \leqslant 0.15\mathrm{Re}_\tau$. It is clear that the log decay in small-scale turbulence overlaps with the log region in the mean flow. In fact, the figure seems to indicate that the log region for small-scale turbulence is over a wider range compared to the mean flow.

The value of these constants are expected to depend on the choice of A^+. The values reported here are for $A^+ = 0.005$. The value of α does not appear to change (for example, for $A^+ = 0.001$); however, the intercept does depend on the amount of energy retained in the filtering process. Regardless of the intercept, the above finding indicates that the rate of change of small-scale fluctuations with wall-normal location (i.e., gradient of wall-normal fluctuations with wall-normal location) is inversely proportional to the distance from the wall (far enough away from the wall).

The large-scale variance increases with increasing Reynolds number. This seems to confirm that the value of A^+ should indeed be independent of wall-normal location (at least in the near-wall and logarithmic region). It should be noted that this value of A^+ is a conservative bound on the frequency. In time scale, this corresponds to 200 wall units. The physical significance of 200 wall units as the cut off timescale is obvious. The near-wall streaks in boundary layers, pipes, and channels all last approximately 100 wall-based time units (and is equivalent to 1000 wall units' length scale) and their features are very robust regardless of the type of flow (see reviews [14–16] and references therein). Therefore, the cutoff of 200 wall units essentially captures the energy contained in these near-wall streaks that self-sustain themselves given a certain mean wall shear stress.

The quoted value of A^+ should be considered as frequency bound above which spectral law of the wall is expected to hold. It is possible that at increasing Reynolds numbers, spectral collapse is observed up to lower values of f^+ (i.e., lower frequencies or equivalently wave numbers, which is indeed the case in Fig. 1) due to increasing scale separation between inner and outer scales. In fact, there is also evidence that a cutoff wavelength of 7000 to 10 000 wall units results in the collapse of small-scale turbulence statistics in the near-wall region (see Refs. [16,17]). This length scale is derived from frequency spectra in liaison with Taylor's local hypothesis. Reference [11] used a cutoff wavelength of 7000 wall units, which approximately corresponds to $f^+ \approx 0.001$, to separate the inner and outer scales to measure amplitude modulation. Moreover, recently, Refs. [18,19] showed that the spectral coherence between two probes (one located in the near-wall region and another in the outer region) at high Reynolds numbers reduced to zero at around 7000 wall units, indicating a value of $A^+ = 0.005$ would also not have any coherence. Very recently, the authors of Ref. [20] performed measurements in the Melbourne facility using the Nanoscale Thermal Anemometry Probe (where the measurements are fully resolved) and showed that the spectrum

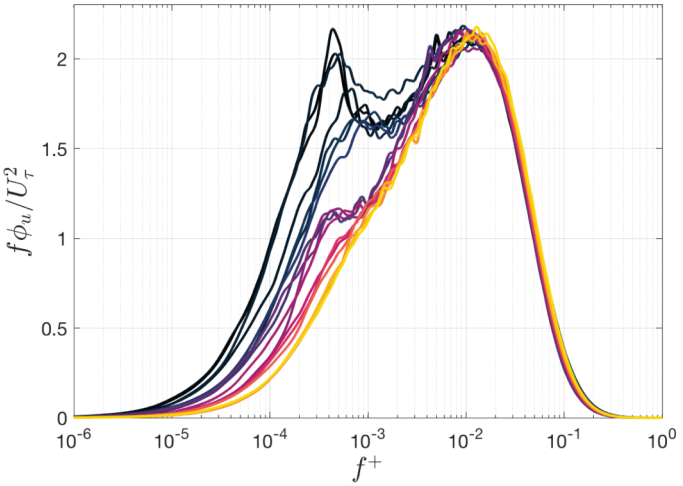

FIG. 3. Inner-normalized premultiplied spectra at $y^+ \approx 15$ for different levels of free-stream turbulence (FST). Lines are colored from lightest to darkest in order of increasing turbulence intensity (the range is from 7% to 13%). The Taylor microscale of FST ranges from 300 to 760. The abscissa shows inner-normalized frequency f^+. Further details on the different turbulence intensities, integral length scales, and boundary layer characteristics can be found in Ref. [21].

indeed collapses with inner scaling across a range of wall-normal positions. In fact, they claim that the collapse is up to wavelengths of 10 000 wall units (that corresponds to approximately 1000 viscous time units) and most certainly up to wavelength of 2000 wall units (200 time units). Therefore, the proposed timescale of 200 wall units is a very conservative estimate for the cutoff frequency above which spectral similarity should hold.

The influence of outer region on the collapse of near-wall high-frequency spectra can be further examined by using data from experiments where the outer influence is artificially enhanced by the introduction of free-stream turbulence. Figure 3 shows spectra obtained at $y^+ = 15$ in an experiment that was designed to increase the strength of outer influence [21–23]. The figure shows the premultiplied power-spectral density (normalized by U_τ) versus inner normalized frequency. In these experiments, the outer influence was exacerbated by using free-stream turbulence and this turbulence intensity would penetrate the boundary layer and alter the mean skin-friction characteristics as well as spectral properties [22]. However, when this altered skin friction is taken into account, the collapse of the spectra at $y^+ = 15$ over a wide range of external forcing is really clear (free-stream turbulence levels up to 13%). It can be seen that for low free-stream turbulence intensity, the collapse is excellent until $f^+ = 0.001$. However, as the FST levels increases, the energetic outer scales penetrate down to the wall and the collapse is worse. Yet, the spectra appear to collapse up to $f^+ = 0.005$ regardless of the intensity of forcing in the outer layer.

IV. CONCLUSIONS

The dimensional analysis approach of Refs. [1,5] to obtain spectral scaling is reinterpreted in the context of experimental observations in high-Reynolds-number turbulent boundary layers. A scaling relation for the high-frequency regime of streamwise energy spectra (in frequency domain) in the near-wall region is proposed based on the hypothesis of law of the wall for the small-scale turbulence intensity. It is noted that the inner scale and Kolmogorov scales are related to each other, yet there are subtle important differences. The inner viscous scale based on U_τ and ν captures the effects of both large and small scales (in the integrated sense). The Kolmogorov scale (η) depends on mean turbulent-kinetic-energy dissipation ($\langle\epsilon\rangle$) and ν where $\langle\epsilon\rangle$ captures the effect of small and large

scales (depending on how much dissipation resides in the low wave numbers or low frequencies). The value of $\langle\epsilon\rangle$ changes with wall-normal location while U_τ does not. Therefore, the value of η and v_η changes with wall-normal location while the inner scales remain fixed. Therefore, the choice of U_τ as the relevant velocity scale and ν/U_τ as the length scale will situate the mean flow and the small-scale turbulence intensity in the same framework. This does not negate Kolmogorov scaling, as other studies have found that the Kolmogorov scales (η and v_η) exhibit universal behavior with inner scaling across different Reynolds numbers.

We observe that when the energy spectra is scaled in inner units, there is a collapse beyond a certain frequency. This value appears to be a universal inner-scaled value across Reynolds numbers. If this was scaled with η, then this value would not be the same for all wall-normal locations. Moreover, the inner-scaled value has a physical significance in that the length scale corresponding to this value is related to the size of the near-wall streaks. The observations here are consistent with the findings related to spectra and Kolmogorov scales in internal and external flows [5,7,20]. In frequency domain, the spectra at similar wall-normal positions are found to collapse down to $f^+ \approx 0.005$ across a whole range of Reynolds numbers. The corresponding small-small turbulence intensity also appears to collapse across all wall-normal positions, confirming the law-of-the-wall hypothesis. The profile follows a logarithmic decay with wall-normal position farther from the wall, which is consistent with Kolmogorov scalings used in Ref. [4]. These observations were further confirmed using experimental data where the boundary layer is under the influence of free-stream turbulence and the collapse of the spectra up to the near-wall streaks appears to be robust.

ACKNOWLEDGMENTS

This study was a reanalysis of existing data and we are grateful to Prof. Marusic and Prof. Hutchins at the University of Melbourne for making the hot-wire data from HRNBLWT available. We thank Dr. Jason Hearst for providing Fig. 3. We are thankful to Prof. Marusic and the anonymous referees for their comments on the manuscript. Financial support of the European Research Council (ERC Grant Agreement No. 277472) and the Engineering and Physical Sciences Research Council of the United Kingdom (EPSRC Grant Ref. No. EP/L006383/1) is gratefully acknowledged.

[1] A. E. Perry and C. J. Abell, Asymptotic similarity of turbulence structures in smooth- and rough-walled pipes, J. Fluid Mech. **79**, 785 (1977).
[2] A. E. Perry and I. Marušić, A wall-wake model for the turbulence structure of boundary layers. Part 1. extension of the attached eddy hypothesis, J. Fluid Mech. **298**, 361 (1995).
[3] A. E. Perry and M. S. Chong, On the mechanism of wall turbulence, J. Fluid Mech. **119**, 173 (1982).
[4] A. E. Perry, S. Henbest, and M. S. Chong, A theoretical and experimental study of wall turbulence, J. Fluid Mech. **165**, 163 (1986).
[5] C. Z. Zamalloa, H. C. H. Ng, P. Chakraborty, and G. Gioia, Spectral analogues of the law of the wall, the defect law and the log law, J. Fluid Mech. **757**, 498 (2014).
[6] J. Schumacher, J. D. Scheel, D. Krasnov, D. A. Donzis, V. Yakhot, and K. R. Sreenivasan, Small-scale universality in fluid turbulence, Proc. Natl. Acad. Sci. USA **111**, 10961 (2014).
[7] S. C. C. Bailey and B. M. Witte, On the universality of local dissipation scales in turbulent channel flow, J. Fluid Mech. **786**, 234 (2016).
[8] V. Yakhot, Probability densities in strong turbulence, Physica D (Amsterdam, Neth.) **215**, 166 (2006).
[9] P. E. Hamlington, D. Krasnov, T. Boeck, and J. Schumacher, Local dissipation scales and energy dissipation-rate moments in channel flow, J. Fluid Mech. **701**, 419 (2012).
[10] N. Hutchins, T. B. Nickels, I. Marusic, and M. S. Chong, Hot-wire spatial resolution issues in wall-bounded turbulence, J. Fluid Mech. **635**, 103 (2009).

[11] R. Mathis, N. Hutchins, and I. Marusic, Large-scale amplitude modulation of the small-scale structures in turbulent boundary layers, J. Fluid Mech. **628**, 311 (2009).
[12] N. Hutchins, J. P. Monty, B. Ganapathisubramani, H. C. H. Ng, and I. Marusic, Three-dimensional conditional structure of a high-Reynolds-number turbulent boundary layer, J. Fluid Mech. **673**, 255 (2011).
[13] I. Marusic, J. P. Monty, M. Hultmark, and A. J. Smits, On the logarithmic region in wall turbulence, J. Fluid Mech. **716**, R3 (2013).
[14] I. Marusic, B. J. McKeon, P. A. Monkewitz, H. M. Nagib, A. J. Smits, and K. R. Sreenivasan, Wall-bounded turbulent flows at high Reynolds numbers: Recent advances and key issues, Phys. Fluids **22**, 065103 (2010).
[15] R. L. Panton, Overview of the self-sustaining mechanisms of wall turbulence, Prog. Aerosp. Sci. **37**, 341 (2001).
[16] A. J. Smits, B. J. McKeon, and I. Marusic, High-Reynolds-number wall turbulence, Annu. Rev. Fluid Mech. **43**, 353 (2011).
[17] I. Marusic, R. Mathis, and N. Hutchins, High Reynolds number effects in wall turbulence, Int. J. Heat Fluid Flow **31**, 418 (2010).
[18] W. J. Baars, N. Hutchins, and I. Marusic, Self-similarity of wall-attached turbulence in boundary layers, J. Fluid Mech. **823**, R2 (2017).
[19] I. Marusic, W. J. Baars, and N. Hutchins, Scaling of the streamwise turbulence intensity in the context of inner-outer interactions in wall turbulence, Phys. Rev. Fluids **2**, 100502 (2017).
[20] M. Samie, I. Marusic, N. Hutchins, M. K. Fu, Y. Fan, M. Hultmark, and A. J. Smits, Fully resolved measurements of turbulent boundary layer flows up to $\mathrm{Re}_\tau = 20\,000$, J. Fluid Mech. **851**, 391 (2018).
[21] R. J. Hearst, E. Dogan, and B. Ganapathisubramani, Robust features of a turbulent boundary layer subjected to high-intensity free-stream turbulence, J. Fluid Mech. **851**, 416 (2018).
[22] E. Dogan, R. E. Hanson, and B. Ganapathisubramani, Effects of large-scale freestream turbulence on turbulent boundary layers, J. Fluid Mech. **802**, 79 (2016).
[23] E. Dogan, R. J. Hearst, and B. Ganapathisubramani, Modelling high Reynolds number wall-turbulence interactions in laboratory experiments using large-scale free-stream turbulence, Philos. Trans. R. Soc. A **375**, 20160091 (2017).